A Water-soluble Warped Nanographene: Synthesis and Applications for Photo-induced Cell Death

Hsing-An Lin,[a,b] Yoshikatsu Sato,* [c] Yasutomo Segawa,* [a,b] Taishi Nishihara,[a,b] Nagisa Sugimoto,[c] Lawrence T. Scott,[d] Tetsuya Higashiyama,[b,c] and Kenichiro Itami* [a,b,c]

Abstract: Nanographene, a small piece of graphene, has attracted unprecedented interest across diverse scientific disciplines particularly in organic electronics. The biological applications of nanographenes, such as bioimaging, cancer therapies and drug delivery, provide significant opportunities for breakthroughs in the field. However, the intrinsic aggregation behavior and low solubility of nanographenes, which stem from their flat structures, hamper their development for bioapplications. Herein, we report a water-soluble warped nanographene (WNG) that can be easily synthesized by sequential regioselective C–H borylation and cross-coupling reactions of the saddle-shaped WNG core structure. The saddle-shaped structure and hydrophilic tetraethylene glycol chains impart high water solubility to the WNG. The water-soluble WNG possesses a range of promising properties including good photostability and low cytotoxicity. Moreover, the water-soluble WNG was successfully internalized into HeLa cells and promoted photo-induced cell death.

Nanographene, a two-dimensional carbon material, has enjoyed widespread application in a variety of electronic and energy devices owing to its extraordinary electronic, optical, and mechanical properties.[1-3] Additionally, the use of nanographene, especially in the form of graphene oxide (GO) and graphene quantum dots (GQDs), in biological applications has recently received tremendous attention. For example, the intense fluorescence emission of GO and GQDs in the ultraviolet to near-infrared region enables their application in biosensing[4,5] and cell imaging.[6,7] Moreover, GO and GQDs have been utilized as stimuli-responsive platforms for drug/gene delivery and photodynamic/photothermal therapy.[7-10] However, the top-down preparation of nanographenes from graphite often results in broad size distributions and degrees of functionalization.[7] Thus, it remains a challenge to precisely tailor the intrinsic properties of nanographene.

The bottom-up chemical synthesis of nanographenes is considered to be a straightforward strategy to prepare nanographene with tunable sizes, shapes, and functionalities.[11,12] Hexa-*peri*-hexabenzocoronene (HBC) is an intensively studied planar nanographene prepared using a bottom-up approach (Figure 1a).[12] Although numerous efforts have been made to engineer the molecular structure of HBC for specific applications,[12] its low solubility and high aggregation tendency in solvents, owing to its planar structure and strong intermolecular π–π interactions,[13] hamper its development. To address the above concerns, lateral substituents or a twist or curvature could be introduced to the structure to impede aggregation.

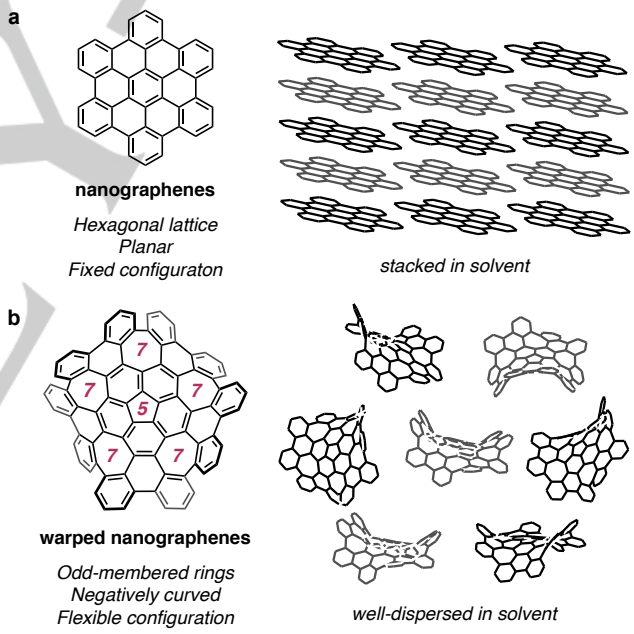

Figure 1. Structures and characteristics of planar nanographenes (a) and warped nanographenes (b).

Nanographene with an embedded three-dimensional, negative Gaussian curvature represents a new class of nanocarbons, which are considered to be next-generation carbon materials.[1,14–23] Due to their saddle-shaped skeletons, negatively curved nanographenes exhibit relatively weak intermolecular π–π interactions and good solubility in organic solvents; they also possess interesting nonlinear optical and electrochemical properties. Recently, we reported a warped nanographene (WNG) with one five-membered ring and five seven-membered rings in the hexagonal lattice (Figure 1b).[22] The negatively curved geometry of this WNG engenders a flexible configuration in solution; as a result, the WNG disperses well in common organic solvents and exhibits green fluorescence. Since curved nanocarbon derivatives are widely

[a] Dr. H.-A. Lin, Dr. T. Nishihara, Prof. Dr. Y. Segawa, Prof. Dr. K. Itami
JST-ERATO, Itami Molecular Nanocarbon Project
Nagoya University
Chikusa, Nagoya 464-8602, Japan
E-mail: ysegawa@nagoya-u.jp (YSe), Itami@chem.nagoya-u.ac.jp (KI)
[b] Dr. H.-A. Lin, Dr. T. Nishihara, Prof. Dr. Y. Segawa, Prof. Dr. T. Higashiyama, Prof. Dr. K. Itami
Graduate Scholl of Science
Nagoya University
Chikusa, Nagoya 464-8602, Japan
[c] N. Sugimoto, Dr. Y. Sato, Prof. Dr. K. Itami
Institute of Transformative Bio-Molecules (WPI-ITbM)
Nagoya University
Chikusa, Nagoya 464-8602, Japan
E-mail: sato.yoshikatsu@i.mbox.nagoya-u.ac.jp (YSa)
[d] Prof. Dr. L. T. Scott
Merkert Chemistry Center
Boston College
Chestunt Hill, Massachusetts 02467-3860, USA

Supporting information for this article can be found under: http://dx.doi.org/10.1002/.

used for cell imaging and photodynamic therapy,[24–26] we envision that WNG could be developed as a new nanoplatform for bioapplications. However, an efficient method of structurally modifying the WNG to generate sufficient hydrophilicity for bioapplications is required. Herein, we report the synthesis of a water-soluble WNG (**7**) by C–H borylation. The fluorescent properties, photostability, and low cytotoxicity of **7** were systematically investigated. Finally, **7** was internalized into HeLa cells and triggered photo-induced cell death upon light stimulation.

The synthetic route to water-soluble WNG **7** is shown in Scheme 1. Because of the synthetic simplicity and ease of diversification, we first synthesized penta-*tert*-butyl WNG (**4**) using our previously reported synthetic route.[22] Pentakis(Bpin)corannulene (**1**), which can be synthesized in one-step from corannulene by C–H borylation,[27] was coupled with 5-*tert*-butyl-2-bromobiphenyl (**2**) using a palladium-catalyzed Suzuki–Miyaura reaction to afford **3** in 98% yield. Intramolecular cyclodehydrogenation (*i.e.*, the Scholl reaction)[28] of **3** using 2,3-dichloro-5,6-dicyanobenzoquinone (DDQ) and trifluoromethanesulfonic acid (TfOH) generated **4** in 50% yield. The structure of **4** was confirmed by X-ray crystallography. Next, iridium-catalyzed C–H borylation[29] of **4** was attempted. Since C–H borylation generally does not occur at the sterically hindered C–H bonds *ortho* to a substituent or ring junction,[29–31] we speculated that **4** would be borylated at the five unhindered C–H positions. Regioselective polyborylation of **5** was carried out in the presence of excess bis(pinacolato)diboron (B_2pin_2), 22 mol % $[Ir(OMe)(cod)]_2$, and 45 mol % 4,4'-di-*tert*-butyl-2,2'-bipyridine (dtbpy) in tetrahydrofuran (THF) at 80 °C. As evidenced by mass spectrometry, the reaction furnished **5** as a major product with small amounts of other intermediates after three days. To complete the borylation reaction, the reaction time was extended to five days; however, the ratio of **5** to the other intermediates in the crude mixture did not change significantly. Finally, **5** was isolated in 76% yield, and its molecular structure was confirmed by X-ray crystal structure analysis.[32] Subsequently, **5** was coupled with bromoarene **6**, which bears three tetra(ethylene glycol) (TEG) chains, by the Suzuki–Miyaura reaction to give **7** in 72% isolated yield. Because of the fifteen hydrophilic TEG chains adding to the curved structure of the WNG core, **7** easily dissolves in a wide range of solvents including non-polar solvents (toluene, chloroform, and diethyl ether), polar aprotic solvents (ethyl acetate, acetonitrile, and dimethyl sulfoxide), and polar protic solvents (methanol and water).

The UV-vis absorption and fluorescence properties of **4** and amphiphilic **7** were examined, and the results are summarized in Figure 2. The two WNG derivatives displayed very similar absorption and emission spectra in dichloromethane (Figure 2a). The maximum absorptions of **4** and **7** appear at 421 and 433 nm, respectively, and their maximum emission appear at 508 and 528 nm, respectively. The absorption and emission peaks of **7** exhibited slight bathochromic shifts compared to those of **4**, which is likely due to the extension of the π-skeleton. In addition, the fluorescence quantum yield of **7** (Φ_F = 0.37) was higher than that of **4** (Φ_F = 0.22). Compound **7** also exhibits positive solvatofluorochromic behavior[33], *i.e.*, the fluorescence spectra shift to a longer-wavelength region in solvents with higher polarity, with good correlation of the $E_t(30)$ values (toluene < dichloromethane < acetonitrile, as shown in Figures S1 and S2); in contrast, the absorption spectra were not affected by the solvent. An aqueous solution of **7** exhibited a slightly broadened absorption spectrum and yellow fluorescence (Φ_F = 0.17, τ = 10.0 ns) (Figure 2b). Compared with Alexa 430 dye, the high photo-stability of **7** in water was confirmed (Figure S3).

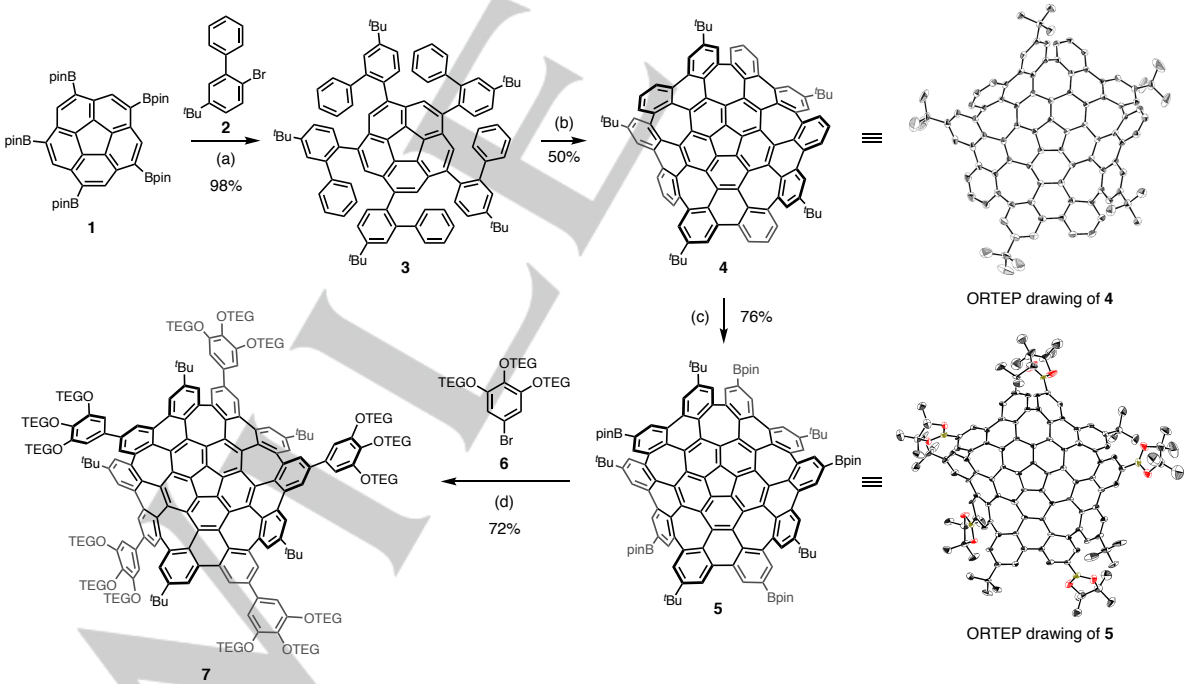

Scheme 1. Synthesis of a water-soluble WNG (**7**). Reaction conditions: (a) **2** (8 equiv), $Pd_2(dba)_3{\cdot}CHCl_3$ (10 mol%), SPhos (20 mol%), Cs_2CO_3 (10.0 equiv), toluene/H_2O (2:1), 80 °C, 24 h; (b) DDQ (11 equiv), TfOH/CH_2Cl_2 (1:9), 0 °C, 1.5 h; (c) B_2pin_2 (11.3 equiv), $[Ir(OMe)(cod)]_2$ (22 mol%) and 4,4'-di-*tert*-butyl-2,2'-bipyridine (45 mol%), 80 °C, 5 days in a Teflon-sealed tube; (d) **6** (10 equiv), $Pd_2(dba)_3{\cdot}CHCl_3$ (10 mol%), SPhos (20 mol%), Cs_2CO_3 (10 equiv), toluene/water (2:1), 80 °C, 48 h. Abbreviations: dba = dibenzylideneacetone; SPhos = 2-dicyclohexylphosphino-2',6'-dimethoxybiphenyl; DDQ = 2,3-dichloro-5,6-dicyanobenzoquinone; TfOH = trifluoromethanesulfonic acid; Bpin = 4,4,5,5-tetramethyl-1,3,2-dioxaborolan-2-yl; TEG = $(CH_2CH_2O)_4Me$. Note: ORTEP drawings are shown with 50% probabilities.

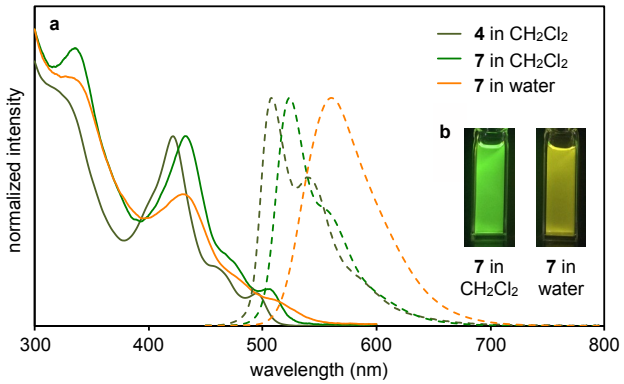

Figure 2. Photophysical properties of functionalized WNGs **4** and **7**. (a) UV–vis spectra (solid line) and fluorescence spectra (broken line) of 4 in CH_2Cl_2 (dark green), **7** in CH_2Cl_2 (green), and **7** in water (orange), ([**4**] or [**7**] = 9.7 x 10^{-6} M). (b) Photographs of the solution of **7** in dichloromethane (left) and water (right) under irradiation at 365 nm.

Exploiting the advantages of **7**, including its high solubility in water, green-yellow fluorescence, and good photostability, we used it to stain live HeLa cells. The biocompatibility of **7** was first evaluated in HeLa cells using the MTT assay. Cell viability was not significantly affected even after treatment with 10 μM of **7** for 24 h (Figure S4), which indicates that **7** has a low cytotoxicity.[34] When the cultured cells were incubated with 5.0 μM **7** for 24 h at 37 °C and then co-stained with 100 nM LysoTracker Red DND-99, green emission was observed from the cells (Figure 3a); and the spots partially overlapped with the red fluorescent signals of the LysoTracker (Figures 3b and 3c). The green emission correlated well with the emission spectrum of the insoluble aggregates generated from the Dulbecco's modified Eagle's medium (DMEM) solution of **7**, and other emission patterns, *e.g.*, the yellow emission of **7** in water or autofluorescence from the cells, were negligible (Figure S5). These results suggest that the water-soluble WNG (**7**) internalized in HeLa cells and accumulated into the lysosome as aggregates.

During live-cell imaging by **7**, we serendipitously discovered that the HeLa cells stained with **7** could be killed by selective laser irradiation. We used a cell-impermeable nucleic acid staining dye, *i.e.*, propidium iodide (PI), as the dead-cell marker and examined the effects of local irradiation with a 489 nm laser on the cell viability of HeLa cells by time-lapse observation. As demonstrated in Figure 4a and Movies 1 and 2, in the presence of 5.0 μM of **7** the light-irradiated HeLa cell shrunk, generated blebs, and finally died. In contrast, no significant changes in the cells were observed under irradiation in the absence of **7**. Moreover, the photodynamic activity and cytotoxicity of **7** in HeLa cells were quantitatively evaluated using various concentrations of **7** (0 to 5 μM). As shown in Figure 4b, the cell viability was ~98% in the presence of 0.01 μM of **7**. Upon increasing the concentration of **7** from 0.01 to 1.0 μM, a dramatic decrease in cell viability was observed, and 91% of the cells were killed in the presence of 1.0 μM **7** under irradiation. Using 5.0 μM **7**, almost no cells survived under the irradiation. In contrast, even in the presence of **7**, no obvious change in cell morphology and viability was observed without light stimulation. Although the mechanism is unclear, the relatively high efficiency of the singlet oxygen generation of **7** (Figures S6,7. See ESI for detail) may contribute to its HeLa cell death.

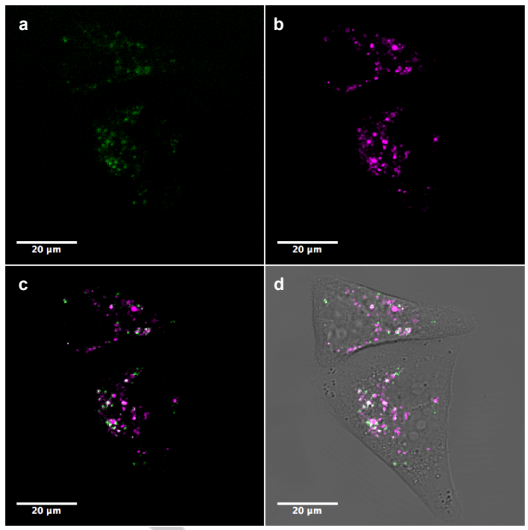

Figure 3. Confocal images of HeLa cells stained with **7** and LysoTracker Red DND-99. Linear unmixing images of (a) **7** and (b) LysoTracker Red DND-99 extracted by reference spectra. (c) Merged image of **7** and LysoTracker Red DND-99 images. (d) Merged image of **7**, LysoTracker Red DND-99 and bright-field images. Cells were excited with a 488 nm laser and the emission spectrum was collected from 490 nm to 693 nm. Unmixing images of background and details of reference spectra are shown in Figure S5.

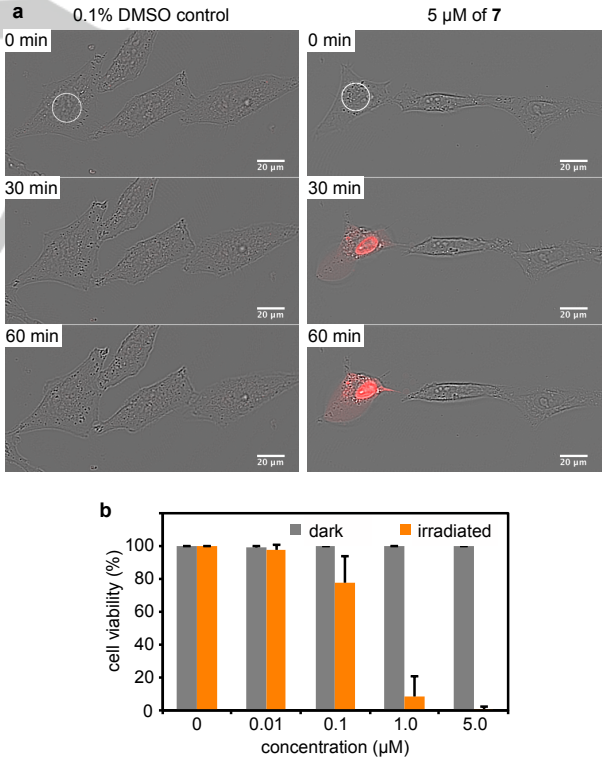

Figure 4. Photodynamic effects of **7** on cell viability. (a) Time-dependent behavior of HeLa cells after local irradiation of a 489 nm light in the presence (right panel) or absence (left panel) of 5 μM **7**. Fluorescence images of propidium iodide (red) excited with a 561 nm laser are overlaid with bright-field images. Open circles indicate the positions of brief irradiation with a 489 nm laser. The time elapsed after irradiation with stimulated light is indicated in the upper left corner. (b) Cell viability of HeLa cells treated with different

concentrations of **7** in the presence or absence of a 489 nm laser irradiation. Fifty cells were analyzed in each experiment, and bars indicate the mean ± standard deviation (SD) from two independent triplicate experiments.

In summary, a water-soluble WNG was successfully synthesized by sequential C–H borylation and cross-coupling of a WNG core. The introduction of hydrophilic tetraethylene glycol chains onto the hydrophobic WNG core generated an amphiphilic water-soluble WNG that can easily disperse in a variety of solvents including polar protic solvents, polar aprotic solvents, and non-polar solvents. Additionally, the water-soluble WNG exhibits green-yellow fluorescence, good photostability, and notably low cytotoxicity to cells. The above favorable properties of this water-soluble WNG enable its use in bioapplications. We demonstrated that the water-soluble WNG was not only readily introduced into HeLa cells, but could also induce cell death upon light irradiation; this is likely due to the photo-induced generation of singlet oxygen from sensitized **7**. Since WNGs can be considered as structurally well-defined GQDs, functionalized WNGs are expected to be developed for a wide range of applications for photodynamic therapy[8-10] in the near future.

Acknowledgements

This work was supported by the ERATO program from JST (JPMJER1302 to K.I.), the Funding Program for KAKENHI from MEXT (JP16K05771 to Y.Se.), and Grant-in-Aid for Scientific Research on Innovative Areas “Integrative system of autonomous environmental signal recognition and memorization for plant plasticity” (JP16H06464 to T.H.), “Advanced Bioimaging Support” (JP16H06280 to T.H.), and “π-Figuration” (JP17H05149 to Y.Se.) from JSPS, and the US National Science Foundation (CHE-1149096 to L.T.S.). Dr. Masayasu Taki, Dr. Kakishi Uno, and Mr. Tsugunori Watanabe are acknowledged for the helpful discussion, photostability analysis, and assistance in synthesis, respectively. ITbM is supported by the World Premier International Research Center Initiative (WPI), Japan.

Keywords: Arenes • Polycycles • Warped Nanographenes • Cell death

[1] A. K. Geim, K. S. Novoselov, *Nat. Mater.* **2007**, *6*, 183.
[2] F. Schwierz, *Nat. Nanotech.* **2010**, *5*, 487.
[3] K. S. Novoselov, V. I.Falko, L. Colombo, P. R.Gellert, M. G.Schwab, K. Kim, *Nature* **2012**, *490*, 192.
[4] S. J. Heerema, C. Dekker, *Nat. Nanotech.* **2016**, *11*, 127.
[5] T. Kuila, S. Bose, P. Khanra, A. K. Mishra, N. H. Kim, J. H. Lee, *Biosens. Bioelectron.* **2011**, *26*, 4637.
[6] J.-L. Li, B. Tang, B. Yuan, L. Sun, X.-G. Wang, *Biomaterials* **2013**, *34*, 9519.
[7] S. Zhu, S. Tang, J. Zhang, B. Yang, *Chem. Commun.* **2012**, *48*, 4527.
[8] K. Yang, L. Feng, X. Shi, Z. Liu, *Chem. Soc. Rev.* **2013**, *42*, 530.
[9] Z. M. Markovic, B. Z. Ristic, K. M. Arsikin, D. G. Klisic, L. M. Harhaji-Trajkovic, B. M. Todorovic-Markovic, D. P. Kepic, T. K. Kravic-Stevovic, S. P. Jovanovic, M. M. Milenkovic, D. D. Milivojevic, V. Z. Bumbasirevic, M. D. Dramicanin, V. S. Trajkovic, *Biomaterials* **2012**, *33*, 7084.
[10] J. Ge, M. Lan, B. Zhou, W. Liu, L. Guo, H. Wang, Q. Jia, G. Niu, X. Huang, H. Zhou, X. Meng, P. Wang, C.-S. Lee, W. Zhang, X. Han, *Nat. Commun.* **2014**, *5*, 4596.
[11] Y. Segawa, H. Ito, K. Itami, *Nat. Rev. Mater.* **2016**, *1*, 15002.
[12] J. Wu, W. Pisula, K. Müllen, *Chem. Rev.* **2007**, *107*, 718.
[13] J. Wu, J. Li, U. Kolb, K. Müllen, *Chem. Commun.* **2006**, 48.
[14] A. Narita, X.-Y. Wang, X. Feng, K. Mullen, *Chem. Soc. Rev.* **2015**, *44*, 6616.
[15] K. Yamamoto, T. Harada, M. Nakazaki, T. Naka, Y. Kai, S. Harada, N. Kasai, *J. Am. Chem. Soc.* **1983**, *105*, 7171.
[16] K. Yamamoto, Y. Saitho, D. Iwaki, T. Ooka, *Angew. Chem. Int. Ed. Engl.* **1991**, *30*, 1173.
[17] C.-N. Feng, M.-Y. Kuo, Y.-T. Wu, *Angew. Chem. Int. Ed.* **2013**, *52*, 7791.
[18] Y. Sakamoto, T. Suzuki, *J. Am. Chem. Soc.* **2013**, *135*, 14074.
[19] R. W. Miller, A. K. Duncan, S. T. Schneebeli, D. L. Gray, A. C. Whalley, *Chem. Eur. J.* **2014**, *20*, 3705.
[20] K. Y. Cheung, X. Xu, Q. Miao, *J. Am. Chem. Soc.* **2015**, *137*, 3910.
[21] I. R. Marquez, N. Fuentes, C. M. Cruz, V. Puente-Munoz, L. Sotorrios, M. L. Marcos, D. Choquesillo-Lazarte, B. Biel, L. Crovetto, E. Gomez-Bengoa, M. T. Gonzalez, R. Martin, J. M. Cuerva, A. G. Campana, *Chem. Sci.* **2017**, *8*, 1068.
[22] K. Kawasumi, Q. Zhang, Y. Segawa, L. T. Scott, K. Itami, *Nat. Chem.* **2013**, *5*, 739.
[23] K. Kato, Y. Segawa, L. T. Scott, K. Itami, *Chem. Asian J.* **2015**, *10*, 1635.
[24] K. Yang, Z. Liu, in *Biomedical Nanomaterials*, Wiley-VCH Verlag GmbH & Co. KGaA, **2016**, pp. 251.
[25] S. Liu, D. Lu, X. Wang, D. Ding, D. Kong, Z. Wang, Y. Zhao, *J. Mater. Chem. B*, **2017**, *5*, 4718.
[26] P. Mroz, G. P. Tegos, H. Gali, T. Wharton, T. Srna, M. R. Hamblin, *Photochem. Photobiol. Sci.* **2007**, *6*, 1139.
[27] M. N. Eliseeva, L. T. Scott, *J. Am. Chem. Soc.* **2012**, *134*, 15169.
[28] M. Grzybowski, K. Skonieczny, H. Butenschön, D. T. Gryko, *Angew. Chem. Int. Ed.* **2013**, *52*, 9900.
[29] I. A. I. Mkhalid, J. H. Barnard, T. B. Marder, J. M. Murphy, J. F. Hartwig, *Chem. Rev.* **2010**, *110*, 890.
[30] T. Ishiyama, J. Takagi, K. Ishida, N. Miyaura, N. R. Anastasi, J. F. Hartwig, *J. Am. Chem. Soc.* **2002**, *124*, 390.
[31] D. N. Coventry, A. S. Batsanov, A. E. Goeta, J. A. K. Howard, T. B. Marder, R. N. Perutz, *Chem. Commun.* **2005**, 2172.
[32] CCDC 1576971 (**4**) and 1576972 (**5**) contain the supplementary crystallographic data for this paper. These data are provided free of charge by The Cambridge Crystallographic Data Centre.
[33] C. Reichardt, *Chem. Rev.* **1994**, *94*, 2319.
[34] C. M. Sayes, A. M. Gobin, K. D. Ausman, J. Medez, J. L. West, V. L. Colvin, *Biomaterials* **2005**, *26*, 7587.

COMMUNICATION

A water-soluble warped nanographene was easily synthesized by sequential regioselective C–H borylation and cross-coupling reactions of the saddle-shaped WNG core structure. The water-soluble warped nanographene was successfully internalized into HeLa cells and promoted photo-induced cell death.

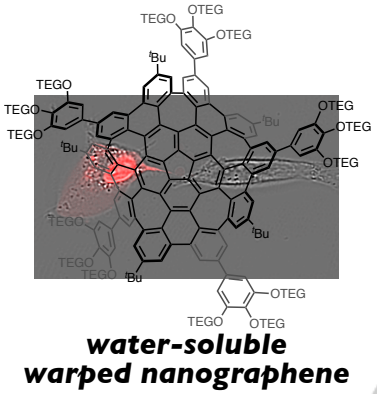

water-soluble warped nanographene

Hsing-An Lin, Yoshikatsu Sato, Yasutomo Segawa,* Taishi Nishihara, Nagisa Sugimoto, Lawrence T. Scott, Tetsuya Higashiyama, and Kenichiro Itami**

Page No. – Page No.

A Water-soluble Warped Nanographene: Synthesis and Applications for Photo-induced Cell Death